

SYMBOLIC DYNAMICS APPLIED IN THE IDENTIFICATION OF FLOW PATTERNS INSIDE TUBE BANKS

Alexandre Vagtinski de Paula and Sergio Viçosa Möller
Universidade Federal do Rio Grande do Sul - UFRGS
Rua Sarmento Leite, 425, 90050-170, Porto Alegre, RS, Brazil
depaula@ufrgs.br; svmoller@ufrgs.br

ABSTRACT

This paper presents a study of the flow patterns identification inside a tube bank with the technique of symbolic dynamics. Experimental signals of mean velocity and its fluctuations are measured by means of hot wire anemometry in an aerodynamic channel and used as input data for the symbolic dynamics technique. The tube bank consists of 23 circular cylinders in triangular arrangement. The pitch-to-diameter ratio chosen was 1.26 and the Reynolds numbers are in the range from 7.5×10^3 to 4.4×10^4 , computed with the tube diameter, $D = 25.1$ mm, and the percolation velocity. In this work, a binary alphabet was chosen to convert and analyze the data. The partitioning process is performed through the mean value of the time series and via discrete wavelet reconstruction, according to a chosen reconstruction level. Results of the flow patterns are presented for different positions inside the tube bank, where histograms and probability density functions support the statistical interpretation. The results of the histograms with decimal representation for the original experimental time series with partitioning performed through the mean value show that the signals do not present fast changes of velocity fluctuations. This behavior was observed in the five rows of cylinders. However, by changing the partitioning according to a wavelet reconstruction of the signal with high frequency, which means that the signals are close to the partitioning function, fast changes appear in all of the time series observed. The results indicate that the turbulence in tube banks has chaotic characteristics.

KEYWORDS

Tube banks, turbulent flow, symbolic dynamics, flow patterns

1. INTRODUCTION

Banks of tubes are found in several engineering applications, like nuclear and process industries, being the most common geometry used in heat exchangers. Tube banks are the usual simplification for fluid flow and heat transfer in the study of shell-and-tube heat exchangers, where the coolant is forced to flow transversely to the tubes by the action of baffle plates. The characterization of the geometry of a tube bank is made by the P/D -ratio, being D the tube diameter and P , the pitch, which is the distance between the centerlines of adjacent tubes. Also, the arrangement of the tubes plays an important role in the characterization of fluid flow and heat transfer of a tube bank

The need for more efficient heat exchangers leads the operating conditions of these equipments to become critical, due to the reduction of the aspect ratio of the tube banks (pitch-to-diameter ratio) and the increasing of the flow velocity. As a consequence of the reduction of the flow area in the narrow gaps between the tubes, which causes velocity fluctuations, and the constant change of the flow direction, static and dynamic loads will be increased [1]. According to [2], the dynamic loads of the turbulent flow over small aspect ratio tube banks are characterized by broad band turbulence, without a defined

shedding frequency. For large aspect ratio tube banks, the dynamic loads are basically associated with a vortex shedding process.

The cross flow passing a tube in a bank is strongly influenced by the presence of the neighboring tubes. In the narrow gap between two tubes in a row, the strong pressure gradient will influence not only the flow in that region, but the flow distribution downstream of this point, in the narrow gap between two tubes in the next row, and so on. The flow through tube banks with staggered arrays to the flow in a curved channel with periodically converging and diverging cross-sections were compared by [3]. For in-line arrays, the comparison is made with a straight channel, being the velocity distribution strongly influenced by the velocity in the narrow gaps.

The leading feature of flow-induced vibration in tube banks is the randomness of dynamic responses of tubes, and even if the tubes are all of equal size, have the same dynamic characteristics, are arranged in regular equidistant rows and are subjected to a uniform steady flow, the dynamic response of tubes is non-uniform and random [4].

Flow induced vibrations mechanisms are usually categorized in turbulent buffeting, vortex shedding acoustic resonance and fluidelastic instability. Recently, bi stable flow is emerging as a possible additional mechanism [5]. For tube banks with square arrangement, bistability forms three-dimensional flow patterns [6] while in triangular array tube banks, the process is mostly two dimensional [7].

Experimental technique used in turbulent flow analysis lead to time series which are usually analyzed by means of Fourier transforms and, more recently with wavelets, e.g. [5, 6], which main feature is the representation of certain phenomenon in time-frequency domain, allowing to observe the behavior of frequency along time and mostly, the features of unsteady flows. The wavelet analysis can be applied to time varying signals, where the stationary hypothesis cannot be maintained, to allow the detection of non-permanent flow structures. A discrete wavelet transform (DWT) is used to make a multilevel decomposition of a time signal in several bandwidth values, accordingly with the selected decomposition level.

From two extensive papers on normal triangular tube arrays and P/D -ratio about the same value of this paper present spectral analysis after the tube rows with hot wire anemometry [8, 9] some conclusions can be drawn: A clear alternate vortex shedding behind the first tube row was found. Near the second row, the spectral peak associated with this excitation has its largest amplitude. Further downstream, the magnitudes of the velocity fluctuations were smaller and uncorrelated in space or time [8]. When the P/D is reduced, the energy of velocity fluctuations with small scales (large Strouhal numbers) is increased, while the highest values of cross-correlations between velocity and pressure fluctuations were found at $P/D = 1.26$ [9].

On the other side, the use of symbolic dynamic technique can allow the extraction and identification of patterns in the flow through the analysis of a particular partition of a time series by means of sequences of abstract symbols, like an alphabet, and the further study of histograms. It is possible to develop a study of topological attractors using a completely different approach, based on symbolic dynamics [10]. A symbolic dynamics technique was applied to extract from chaotic signals of turbulent fluctuations data, information related to the structure of unstable periodic orbits [11]. The authors concluded that their methodology could be applied in the analysis of fluctuations in turbulent data measured experimentally.

A simplified method of symbolization of experimental time series, as well as its use in describing a two-dimensional Poincaré section discretized was presented by [12]. A comprehensive review of a symbolic dynamics technique to study the dynamics of economic systems was presented by [13]. A symbolic analysis of time series data from multidimensional measuring to identify patterns in dynamic systems was

presented by [14]. Thus, the study of attractors based on symbolic dynamics involves the analysis and characterization of the time series using statistical density histograms representative of symbolic sequences. This tool is also useful to measure complexity in coded sequences [13].

2. OBJECTIVES

The use of symbolic dynamics of the turbulent cross flow over tube banks can be applied not only to experimental time series, but also on the reconstructed attractor in the state space, aiming at identifying patterns contained within the data.

The purpose of this paper is, therefore, to study the turbulent cross flow over a tube bank of five rows of circular cylinders placed in an aerodynamic channel. Through the technique of symbolic dynamics applied to the experimental time series, a decimal representation is performed through histograms according to a binary alphabet. The partitioning process is performed through the mean value of the time series and via discrete wavelet reconstruction, according to a chosen reconstruction level.

3. METHODOLOGY

Experimental time series of axial velocity of the flow are obtained with the constant temperature hot wire anemometry technique in an aerodynamic channel and are used as input data in a dynamic symbolic approach, enabling the analysis of the data. The average speed and speed fluctuations of the air are measured downstream the tubes. Wavelet transforms were also applied to perform a joint time-frequency domain analysis of the experimental signals, in order to make a multilevel decomposition of the signals in several bandwidth values, accordingly with the selected decomposition level.

3.1. Experimental technique

The aerodynamic channel used in the experiments is made of acrylic, with a rectangular test section of 0.146 m height, width of 0.193 m and 1.02 m of length (Fig. 1a). The air is impelled by a centrifugal blower of 0.64 kW, and passes through two honeycombs and two screens, which reduce the turbulence intensity to about 1% in the test section. Upstream the test section, placed in one of the side walls, a Pitot tube measures the reference velocity of the non-perturbed flow.

The velocity of the flow and its fluctuations are measured by means of a DANTEC *StreamLine* constant hot-wire anemometry system. A single straight hot wire probe (type DANTEC 55P11) was used in the experiments. Data acquisition is performed by a 16-bit A/D-board (NATIONAL INSTRUMENTS 9215-A) with USB interface. The acquisition frequency of time series was of 1 kHz, and a low-pass filter of 300 Hz was used to avoid aliasing.

The circular cylinders, with external diameter of 25.1 mm, are made of Polyvinyl chloride (PVC), are rigidly attached to the top wall of test section and their extremities are closed. The probe support is positioned with 3D transverse system placed 200 mm downstream the outlets (Fig. 2b). The mean error of the flow velocity determination with a hot wire was about +/- 3%. The Reynolds numbers are in the range from 7.5×10^3 to 4.4×10^4 , computed with the diameter of the circular cylinders and the percolation velocity.

Figure 2 shows a schematic top view of the tube bank with the 23 circular cylinders and probe positions, which was aligned along the tangent to the external generatrices of the tubes.

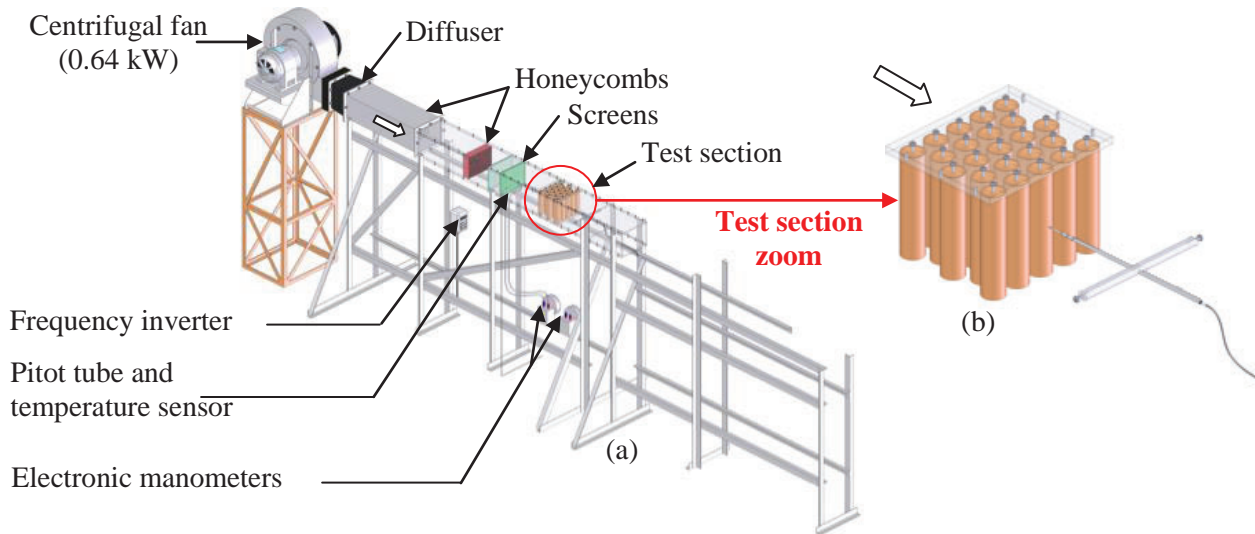


Figure 1. Schematic view of (a) the aerodynamic channel, (b) test section.

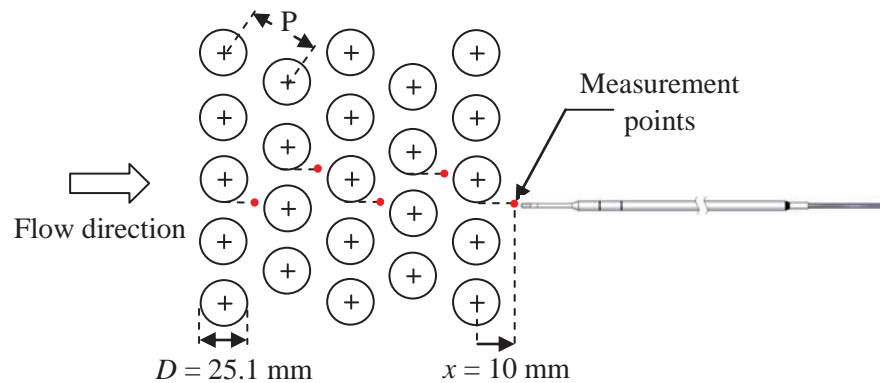


Figure 2. Schematic top view of the experiment and probes positions.

3.2. Wavelet transforms

The wavelet analysis can be applied to time varying signals, where the stationary hypothesis cannot be maintained, to allow the detection of non-permanent flow structures. The Fourier transform of a discrete time series gives the energy distribution of the signal in the frequency domain evaluated over the entire time interval. While the Fourier transform uses trigonometric functions as basis, the lowers of wavelet transforms are functions named wavelets, with finite energy and zero average that generates a set of wavelet basis. The continuous wavelet transform of a function $x(t)$ is given by

$$\tilde{X}(a,b) = \int_{-\infty}^{\infty} x(t) \psi_{a,b}(t) dt, \quad (1)$$

where ψ is the wavelet function and the parameters a and b are respectively scale and position coefficients ($a, b \in \Re$) and $a > 0$. The respective wavelet spectrum is defined as

$$P_{xx}(a,b) = |\tilde{X}(a,b)|^2. \quad (2)$$

In the wavelet spectrum, Eq. (2), the energy is related to each time and scale (or frequency) [15]. This characteristic allows the representation of the distribution of the energy of the signal over time and frequency domains, called spectrogram. The discrete wavelet transform (DWT) is a judicious sub sampling of the continuous wavelet transform (CWT), dealing with dyadic scales, and given by [16]

$$d(j, k) = \sum_t x(t) \psi_{j,k}(t), \quad (3)$$

where the scale and position coefficients ($j, k \in \mathbb{I}$) are dyadic sub samples of (a, b). Any discrete time series with sampling frequency F_s can be represented by

$$x(t) = \sum_k c(J, k) F_{J,k}(t) + \sum_{j \leq J} \sum_k d(j, k) y_{j,k}(t), \quad (4)$$

where the first term is the approximation of the signal at the scale J , which corresponds to the frequency interval $[0, F_s/2^{J+1}]$ and the inner summation of the second term are details of the signal at the scales j ($1 \leq j \leq J$), which corresponds to frequency intervals $[F_s/2^{j+1}, F_s/2^j]$. The velocity signals were analyzed using discrete wavelet transforms to decompose the measured signal in wavelet approximations divided in frequency bands [17].

In this work, Daubechies Db20 functions were used as lowers of discrete wavelet transforms. A study of wavelet transforms applied to accelerating and decelerating turbulent flows in tube banks can be found in [17]. Mathematical tools were developed using Matlab[®] software and its specific toolboxes for statistical, spectral and wavelet analysis.

3.3. Symbolic dynamics

The technique of symbolic dynamics applied to the experimental series in this work is the same as proposed by [12]. The steps used in this procedure are as follows:

- (a) the time series data is divided (or partitioned) into a convenient position;
- (b) the values of the time series are converted according to the alphabet chosen, containing n symbols, based on the partitioning performed, generating a symbolic series;
- (c) a length k is chosen to represent words, being generated m words, where $m = n^k$;
- (d) a transformation is performed in decimal representation of words generated.

The necessary steps described above for the symbolization of time series to construct the histogram of symbolic sequences are shown schematically in Fig. 3.

The result is displayed using histograms according to the decimal representation (Fig. 4a). This result represents the statistical density of symbolic sequences, where the horizontal axis represents the symbolic sequences and the vertical axis the absolute or relative frequency of the sequences.

For the binary alphabet, for example, there are two letters (0 or 1), or $n = 2$. If the length for the representation of words was chosen equal 3 ($k = 3$), there will be $m = n^k = 2^3 = 8$ words (000, 001, 010, 011, 100, 101, 110 and 111). The probability of a binary episode i , denoted by p_i , will be between $0 \leq p \leq 1$. A partial representation of a symbolic binary tree for lengths of symbolic sequence k from 1 to 3 is illustrated in Fig. 4b.

For purely random data sequences, all symbolic sequences of length m are equiprobable, that is, the result should have uniform density. Thus, the detachment of such behavior indicates the structure of the deterministic data, that can be chaotic or not.

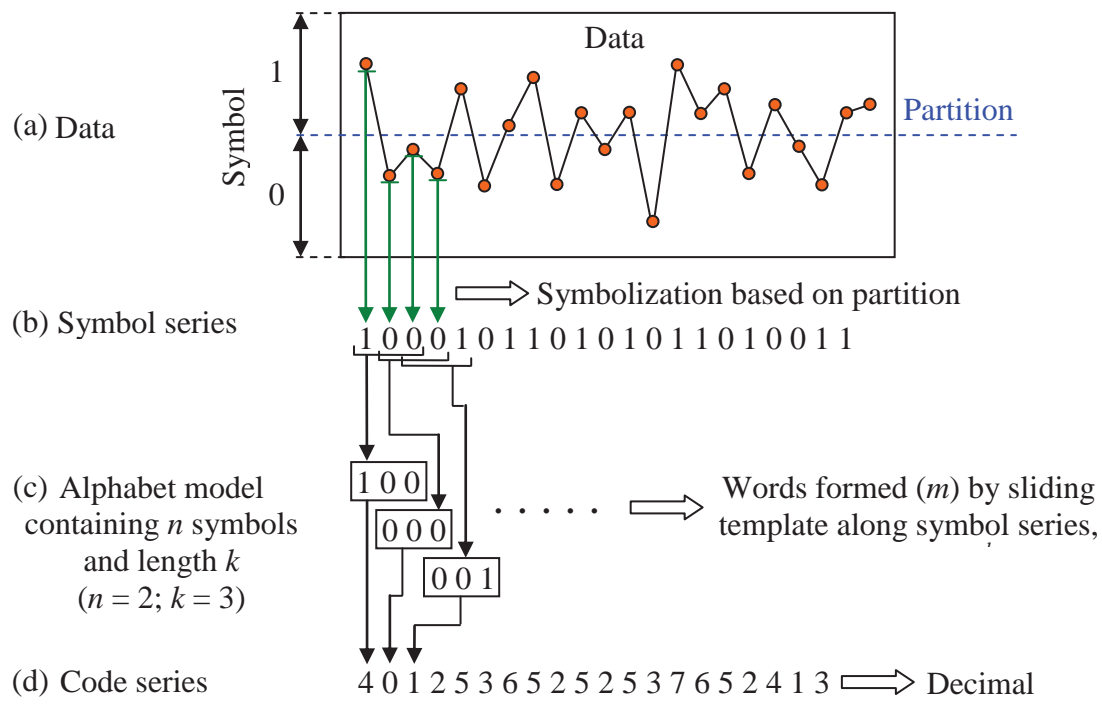


Figure 3. Process symbolizing a series of data to construct the histogram of the symbolic sequence. Adapted from [12].

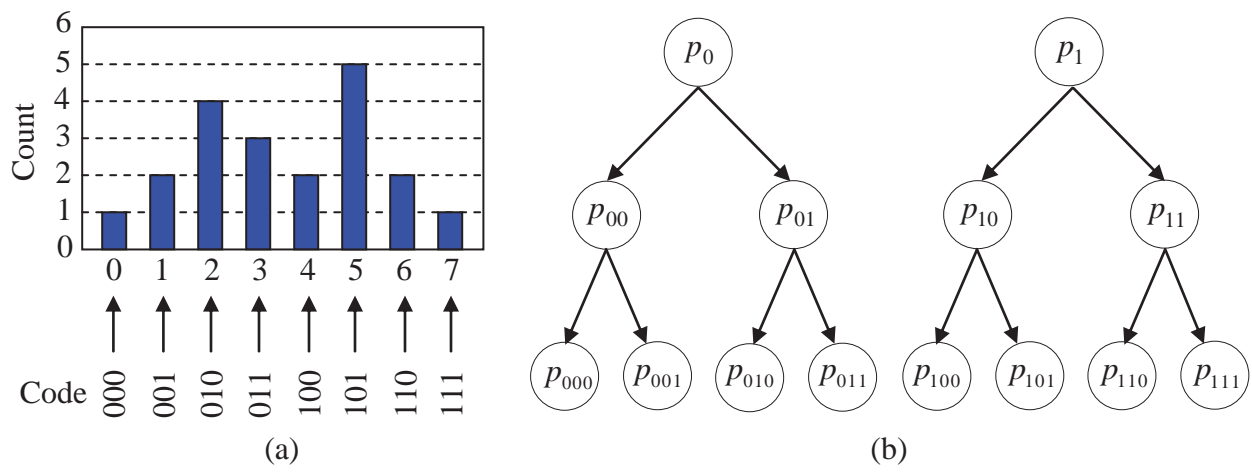


Figure 4. (a) Histogram constructed according to the decimal representation. (b) Partial representation of a symbolic binary tree for lengths of symbolic sequence k from 1 to 3. Adapted from [12].

4. RESULTS

Figure 5 shows the time series of axial velocity after the first, second, third, fourth and fifth rows of cylinders, with its respective probability density functions. The turbulent feature of flow is observed from the data as velocity fluctuations, while the probability density functions (PDF) show a bell-shaped, with small asymmetry and positive skewness. No changes in the gap flow direction were observed. Table I shows the four first moments of the PDF shown in Fig. 5. The shape of the PDF from the second to the fourth rows is similar. For the first and the fifth rows, the PDF is sharper, which can be seen from the lower values of their respective standard deviations in Table I.

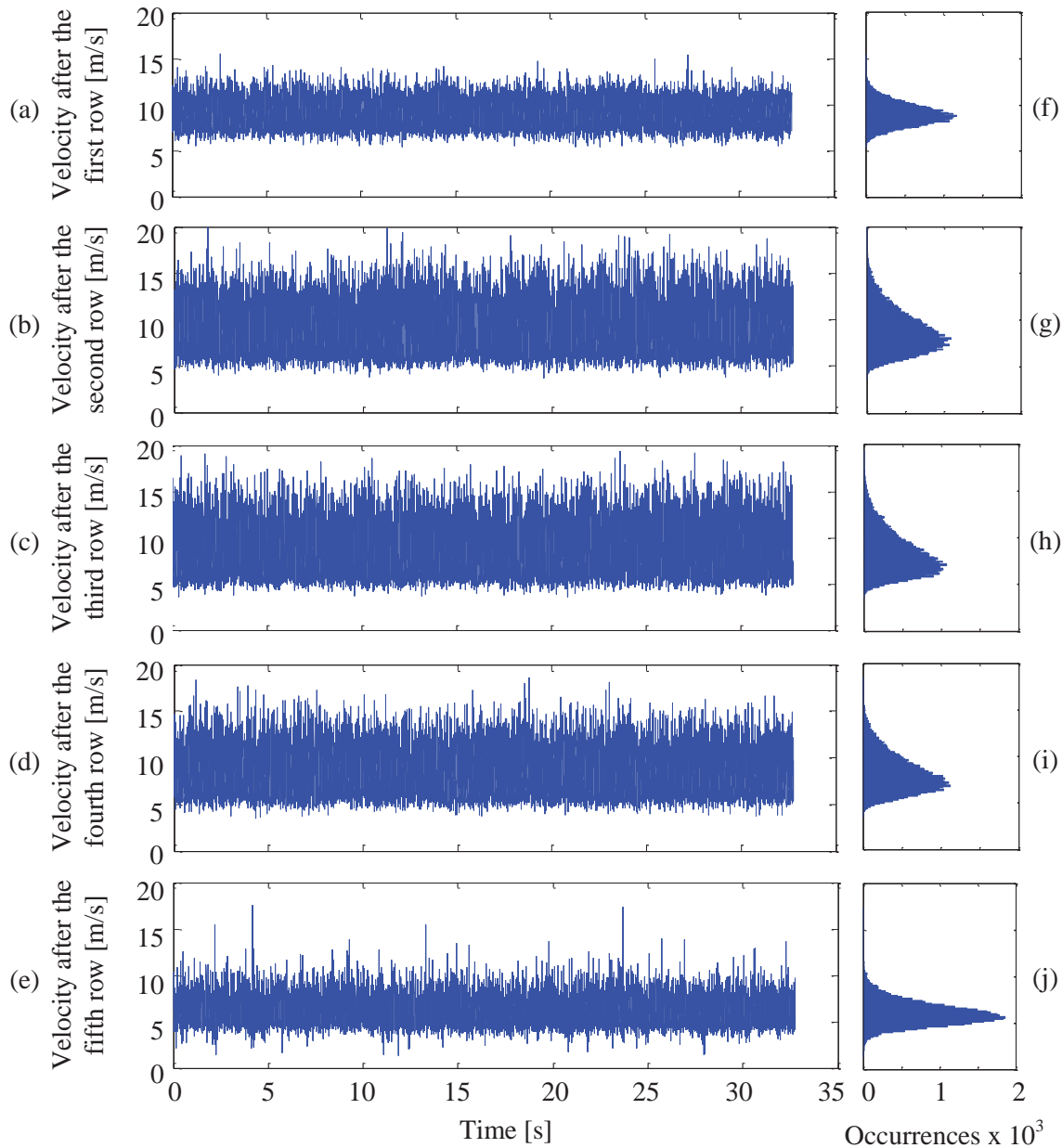


Figure 5. Time series of velocity after the first (a), second (b), third (c), fourth (d) and fifth (e) rows of cylinders, with its respective probability density functions (f-j).

The symbolic dynamics technique was applied to velocity time series of Fig. 5, where each signal is partitioned in its mean value. A binary alphabet ($n = 1$) and initially only two words were used ($k = 1$, $m = n^k = 2^1 = 2$ words (0 and 1, in binary alphabet). The results are shown in Fig. 6, where a higher relative frequency (occurrence) of the word 0 is observed, meaning there is a larger number of data points below the average value of the time series. Such evidence was expected, since according to the PDF, all time signals have positive skewness.

Table I. Four moments of the PDF shown in Fig. 5.

Row #	1	2	3	4	5
Mean velocity [m/s]	9.02	8.89	8.40	8.25	6.09
Standard deviation [m/s]	1.49	5.16	5.42	4.26	1.76
Skewness	3.26	3.45	3.61	3.54	6.31
Kurtosis	0.39	0.75	0.88	0.81	0.98

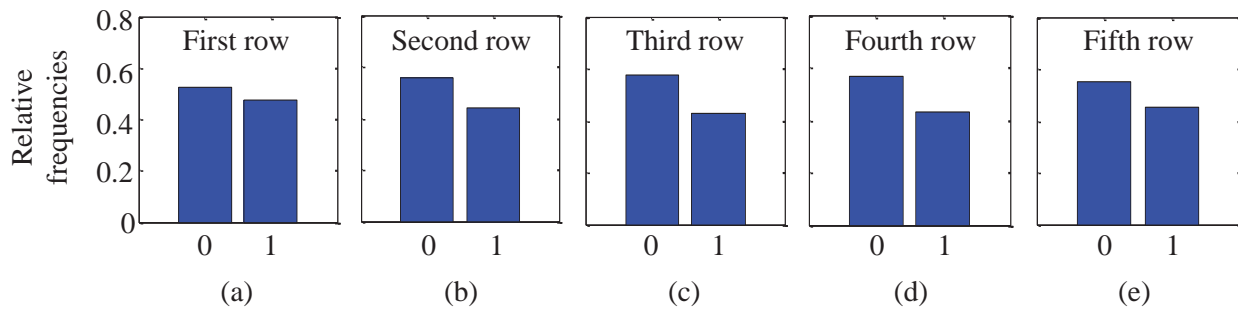


Figure 6. Relative frequencies of the time series with binary alphabet and only two words ($k = 1$). Results from the first to fifth rows of cylinders (a-e, respectively).

Table II shows the numerical values of the relative frequencies of Fig. 6, which shows that its value for the symbol 0 increases as it enters the tube bank until the third row (middle of the bank) and then decreases, opposite behavior to that observed for the symbol 1 (higher velocity values).

Table II. Numerical values of the relative frequencies of Fig. 6, with $k = 1$.

Symbol	Row					Relative frequency
	1	2	3	4	5	
0	52.64 %	55.86 %	57.32 %	56.80 %	54.97 %	
1	47.36 %	44.14 %	42.68 %	43.20 %	45.03 %	

The results for the analysis of four words ($k = 2$, $m = n^k = 2^2 = 4$ words (00, 01, 10 and 11, in binary alphabet) are shown in Fig. 7, where a similar behavior is observed from the histograms, with a decrease of the intermediate relative frequencies, in decimal 1 and 2, (words "01" and "10" of the binary alphabet). This indicates that there is a smaller number of fast changes of velocity values of the signals, when the signal is with its value below the average value of the series, there is less occurrence of changes to values higher than the average (0 to 1). The same occurs with the signal starting with its initial value above the average (from 1 to 0).

Table III shows the numerical values of the relative frequencies of Fig. 7. Again, the value for the extreme of the alphabet (symbol 00) increases as it enters the tube bank until the third row and then decreases. One interesting feature observed in the data is that the occurrences of the intermediate values (words "01" and "10" of the binary alphabet) are identical.

For more words in the alphabet (8, 16 and 32 words), results are shown in Fig. 8 for the first row of cylinders. The partitioning through the mean value produces more occurrences in the extremes of the alphabet, showing that long sequences of higher or lowest values in respect to the mean are more probable in the time series. For example, in Fig. 8b, for $k = 4$ (16 words), the occurrences of the words "0101" or "1010" appears about ten times less than the sequence "0000", showing that very fast changes in velocity directions of the flow are less probable. This means that long sequences containing "ones" and "zeros" are less probable than other sequences. Similar results are obtained for the other time series, from the second to the fifth row of cylinders.

As an alternative to partitioning around the mean value of the series, a partitioning with discrete wavelet transform of the original signal was performed. As an example of the application of this partitioning, Fig. 9a shows the first five seconds of the time series after the first row of cylinders with its reconstruction via discrete wavelet transform of level $j = 5$ (frequencies from 0 to 15.625 Hz), with its respective probability density functions (Fig. 9b). The PDF of the reconstructed signal is also bell-shaped but with lower amplitude in velocity, as expected.

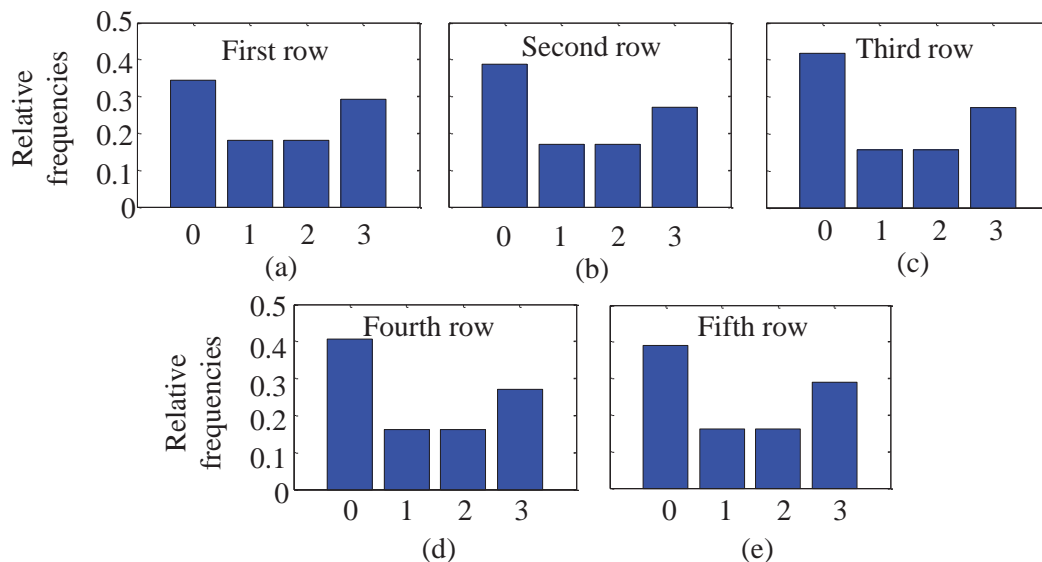


Figure 7. Relative frequencies of the time series with binary alphabet and four words ($k = 2$). Results from the first to fifth rows of cylinders (a-e, respectively).

Table III. Numerical values of the relative frequencies of Fig. 7, with $k = 2$.

Symbol	Row					Relative frequency
	1	2	3	4	5	
00	34.48 %	38.84 %	41.81 %	40.64 %	38.91 %	
01	18.16 %	17.02 %	15.51 %	16.16 %	16.07 %	
10	18.16 %	17.02 %	15.51 %	16.16 %	16.06 %	
11	29.20 %	27.12 %	27.17 %	27.04 %	28.96 %	

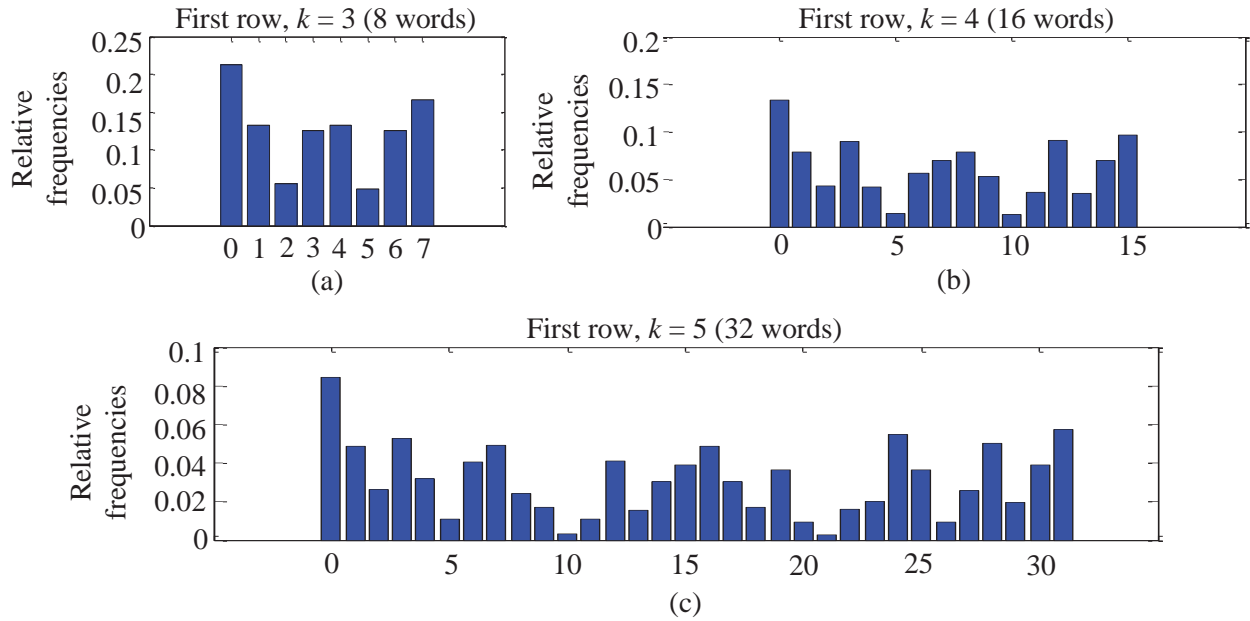


Figure 8. Relative frequencies of the time series after the first row of cylinders with binary alphabet. (a) $k = 3$ or 8 words, (b) $k = 4$ or 16 words and (c) $k = 5$ or 32 words.

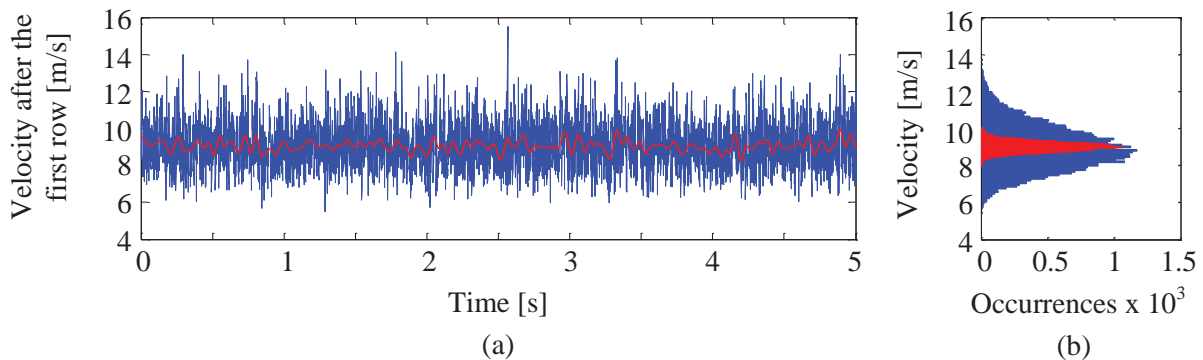


Figure 9. (a) First five seconds of the time series (in blue color) after the first row of cylinders with its reconstruction via discrete wavelet transform (in red color) of level $j = 5$ (frequencies from 0 to 15.625 Hz), with its respective probability density functions (b).

The histograms obtained with the result of symbolic dynamics analysis are shown in Fig. 10, for binary alphabet and $k = 4$ (16 words) and reconstruction levels of $j = 9$, $j = 7$, $j = 5$, $j = 3$ and $j = 1$. Since the partitioning that filters the signal for a low frequency range ($n = 9$, Fig. 10a) until the partitioning with reconstructions for higher frequencies ($j = 1$, Fig. 10e), the number of occurrence of the ends of the histograms decreases. By the partitioning performed with $j = 9$ to $j = 3$ (Figs. 10a to 10d), word “5” (0101) and word “10” (1010) appears in smaller amounts.

For partitioning performed with $j = 1$ (Fig. 10e), a minimum is found for different words. The words "0" (0000) and "15" (1111) does not appear in the histogram. There is also little occurrence of the words "1" (0001), "7" (0111), "8" (1000) and "14" (1110). This is due to the fact that the partitioning function selected (via reconstruction of DWT of high frequency) is close to the time series, which allows rapid flow fluctuations through the partitioning function, with no more than three consecutive data point above or below it, for the sampling frequency used in the measurement of the data ($F_s = 1000$ Hz). This finding suggests that the analysis of the behavior of the velocity fluctuations through a special partitioning, as the discrete wavelet reconstruction, can be improved by this technique.

To observe this behavior in more details, Fig. 11a shows the first 0.2 seconds of the time series after the first row of cylinders together with their reconstruction via DWT of level $j = 1$ (Fig. 11b). The detail vector via DWT is shown in Fig. 11c, which is used in the partitioning of the time series. The symbolization process of the velocity signal with binary alphabet (Fig. 11d) presents fast changes between the state "0" and "1". Other levels of reconstruction, wavelet function or partitioning positions can be used to extract more information hidden in the experimental raw data.

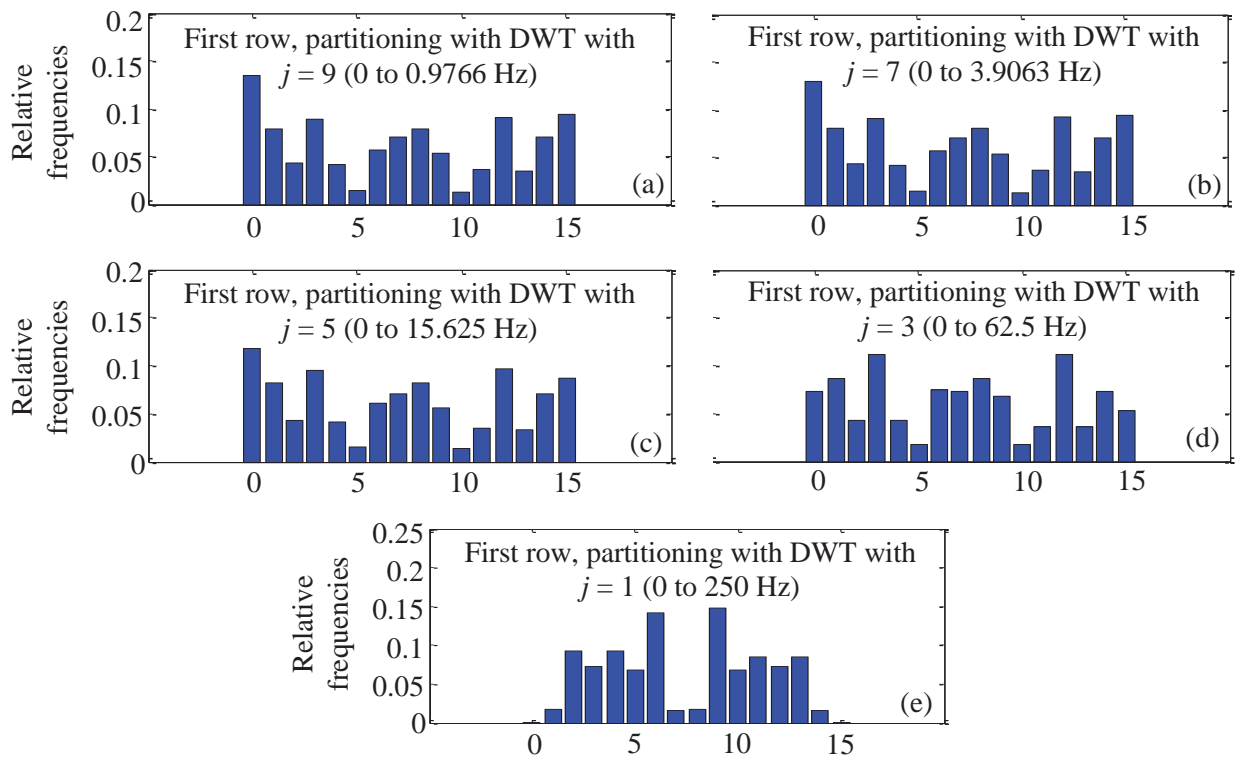


Figure 10. Relative frequencies of the time series after the first row of cylinders with binary alphabet and partitioning performed through reconstructions from DWT of the signals. Reconstruction levels: (a) $j = 9$, (b) $j = 7$, (c) $j = 5$, (d) $j = 3$ and (e) $j = 1$.

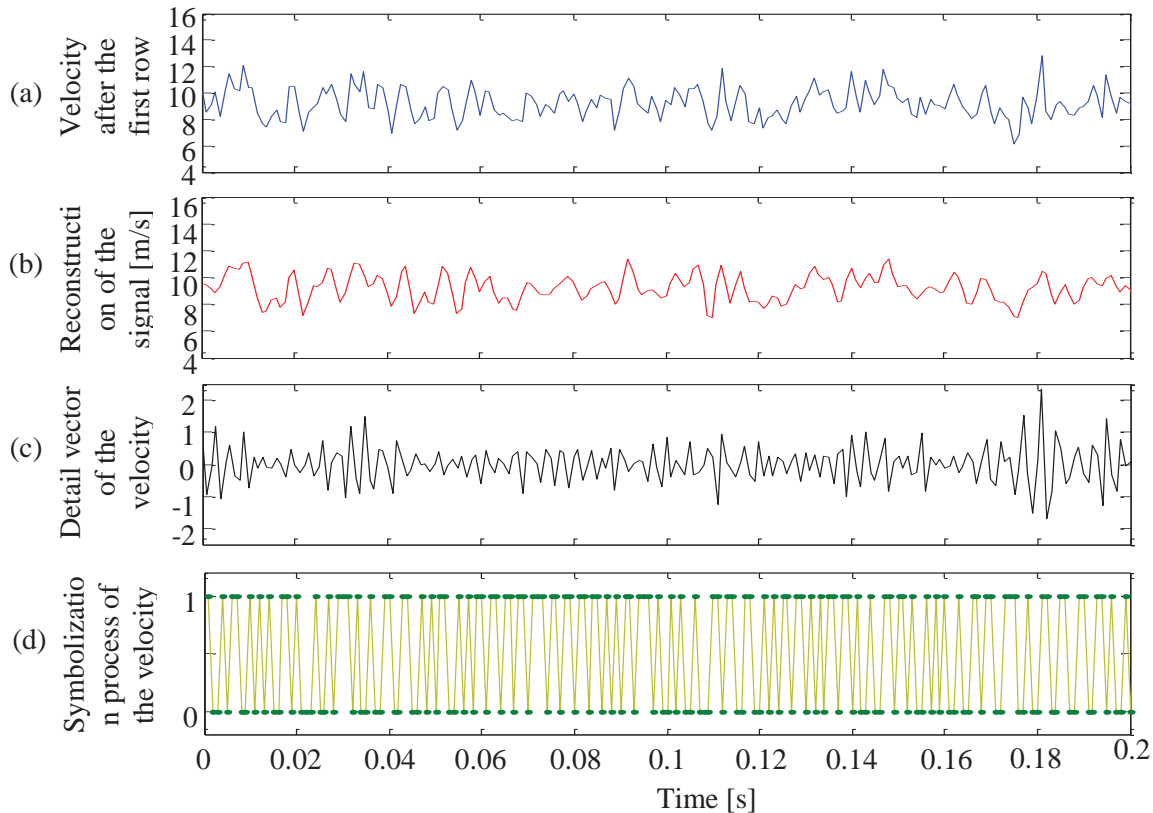


Figure 11. (a) First 0.2 seconds of the time series after the first row of cylinders. (b) Reconstruction via DWT of level $j = 1$ (frequencies from 0 to 250 Hz). (c) Detail vector via DWT. (d) Symbolization process of the velocity signal with binary alphabet.

5. CONCLUSIONS

This work presents a study of the application of symbolic dynamics in the turbulent cross flow over a tube bank of five rows of circular cylinders. By means of hot wire anemometry technique time series of velocity are acquired in an aerodynamic channel. The application of symbolic dynamics allows the identification of the flow patterns where the time series are partitioned according to an alphabet. In this work, a binary alphabet was chosen, and the partitioning process was performed through the mean value of the velocity time series and according to reconstructions from discrete wavelet transform of the signals with different levels of reconstruction or frequency band. The results of the histograms with decimal representation for the original experimental time series with partitioning performed through the mean value show that the signals do not present fast changes of velocity fluctuations. This behavior was observed in the five rows of cylinders. However, by changing the partitioning according to a wavelet reconstruction of the signal with high frequency, which means that the signals are close to the partitioning function, fast changes appear in all of the time series observed. This shows that the symbolic dynamics technique can be applied to the identification of high frequency changes of the velocity flow pattern inside tube banks with an appropriated partitioning function. Based on the observation of the histograms, where relative frequencies are not uniform, the results indicate that the turbulence in tube banks have chaotic characteristics.

While spectral analysis delivers the localization of kinetic energy of the flow in frequency domain, the symbolic dynamics gives the analysis of the flow structures for different sizes or words with the time,

being an additional tool to study the flow inside tube banks. Previous results from the literature using classic Fourier analysis could, therefore, be enhanced with the present procedure.

Future works contemplating the use of other alphabets or different partitions are intended. Also, this technique can be applied in the topological study of the time series, by the choosing of a convenient Poincaré section.

ACKNOWLEDGMENTS

Authors gratefully acknowledge the support by the CNPq – National Council for Scientific and Technological Development, Ministry of Science and Technology (MCT), Brazil.

Alexandre V. de Paula thanks also the CNPq for granting him a fellowship.

REFERENCES

1. L. A. M. Endres, C. Silva, S. V. Möller, “Experimental study of static and dynamic fluid flow loads in tube banks”, *Transactions of SMiRT 13*, 13th International conference on structural mechanics in reactor technology, Porto Alegre, Brazil (1995).
2. R. D. Blevins, *Flow Induced Vibrations*, van Nostrand-Reinhold, New York (1990).
3. A. A. Žukauskas, “Heat transfer from tubes in crossflow”, *Advances in heat transfer*, **8**, p. 93-160 (1972).
4. M. M. Zdravkovich and K. L. Stonebanks, “Intrinsically nonuniform and metastableflow in and behind tube arrays”, *Journal of Fluids and Structures*, **4**, No 3, p. 305-319 (1990).
5. D. B. Keogh, C. Meskell. “Bi-stable flow in parallel triangular tube arrays with a pitch-to-diameter ratio of 1.375”, *Nuclear Engineering and Design* 285, pp. 98–108 (2015).
6. C. R. Olinto, L. A. M. Endres, S. V. Moller, “Experimental study of the characteristics of the flow in the first rows of tube banks”. *Nuclear Engineering and Design*, **239**, pp. 2022–2034, (2009).
7. A. V. de Paula, L. A. M. Endres, S. V. Moller, “Bistable features of the turbulent flow in tube banks of triangular arrangement”, *Nuclear Engineering and Design*, **249**, pp. 379– 387 (2012).
8. D. R. Polak and D. S. Wever, “Vortex shedding in normal triangular tube arrays”, *Journal of Fluid and Structures*, **9**, p. 1-17 (1995).
9. L. A. M. Endres and S. V. Möller, “On the fluctuating wall pressure field in tube banks”, *Nuclear Engineering and Design*, **203**, p. 13-26 (2001).
10. N. F. Ferrara and C. P. C. Prado, *Caos: Uma nova introdução*, Editora Edgar Blücher, São Paulo (1999).
11. M. Lehrman and A. B. Rechester, “Extracting symbolic cycles from turbulent fluctuation data”, *Physical Review Letters*, **87**, No. 16, 164501, p. 1-4 (2001).
12. C. S. Daw, C. E. A. Finney and E. R. Tracy, “A review of symbolic analysis of experimental data”, *Review of Scientific Instruments*, **74**, No. 2, p. 915-930 (2003).
13. J. G. Brida and L. F. Punzo, “Symbolic time series analysis and dynamic regimes”, *Structural Change and Economic Dynamics*, **14**, p. 159-183 (2003).
14. V. Rajagopalan, A. Ray, R. Samsi and J. Mayer, “Pattern identification in dynamical systems via symbolic time series analysis”, *Pattern Recognition*, **40**, p. 2897–2907 (2007).
15. I. Daubechies, *Ten Lectures on Wavelets*, Society for Industrial and Applied Mathematics (1992).
16. D. B. Percival and A. T. Walden, *Wavelet Methods for Time Series Analysis*, Cambridge University Press (2000).
17. M. L. S. Indrusiak, J. V. Goulart, C. R. Olinto and S. V. Möller, “Wavelet time–frequency analysis of accelerating and decelerating flows in a tube bank”, *Nuclear Engineering and Design*, **235**, p. 1875-1887 (2005).